Active Photoswitching of Sharp Fano Resonances in THz Metadevices

Manjappa, Manukumara; Srivastava, Yogesh Kumar; Cong, Longqing; Al-Naib, Ibraheem; Singh, Ranjan

2017

Manjappa, M., Srivastava, Y. K., Cong, L., Al-Naib, I., & Singh, R. (2017). Active Photoswitching of Sharp Fano Resonances in THz Metadevices. Advanced Materials, 29(3), 1603355-.

https://hdl.handle.net/10356/83759

https://doi.org/10.1002/adma.201603355

Active Photo-switching of sharp Fano resonances in THz metadevices

Manukumara Manjappa[1,2,], Yogesh Kumar Srivastava[1,2,*], Longqing Cong[1,2,*], Ibraheem Al-Naib[3], and Ranjan Singh[1,2,†]*

[1] *Division of Physics and Applied Physics, School of Physical and Mathematical Sciences, Nanyang Technological University, 21 Nanyang Link, Singapore 637371.*
[2] *Centre for Disruptive Photonic Technologies, The Photonics Institute, Nanyang Technological University, 50 Nanyang Avenue, Singapore 639798.*
[3] *Biomedical Engineering Department, College of Engineering, University of Dammam, Dammam, Saudi Arabia.*
[*] *These authors contributed equally to this work.*
[†] Corresponding author: *ranjans@ntu.edu.sg.*

Keywords: Fano resonance, active control, figure of merit, terahertz metamaterials

Abstract

Fano resonances in metamaterials occur due to the interference effects appearing in the coupled systems and show a great deal of potential in ultrasensitive sensing and nonlinear applications. Moreover, precise and dynamic control of Fano resonances would enhance their implications in the real world technologies in realizing active sensors and ultrafast switchable metadevices. Here, we demonstrate active photo-switching of Fano resonance in a silicon implanted terahertz asymmetric metallic split ring (Si-TASR) metamaterial system at extremely low pump powers. Our results show complete switching off behavior of the Fano resonance at moderate pump powers signifying ultrahigh sensitivity of its near field energy to the external pump illumination. As the pump power is increased, the Fano resonance abates exponentially with increasing photoconductivity of the implanted silicon islands. A basic electrical circuit model is employed to explain the underlying mechanism of the Fano coupling in the proposed system that shows good agreement with our observed experimental results. Besides, the low threshold ultrafast switching behavior of Fano resonances would facilitate the design of metadevices with diverse functional properties such as active sensors, high quality factor modulators, filters, nonlinear devices, and lasing spasers over broad range of frequencies across the electromagnetic spectrum.

I. Introduction

Scattering processes occurring in light-matter interaction are important tools in investigating the resonant and non-resonant optical properties of materials. Nature and strength of the scattering phenomenon are determined by the shape and line-width of the spectral feature that are owed to the absence or presence of interference effects occurring in the system. Typically, the symmetric spectral features described by the Lorentz model result from overlapping of distinct resonances of different origin, whereas the asymmetric spectral features showing the Fano line shape is a consequence of the Fano-type of interference effects in the system. Hence, Fano resonance differs from the fundamental Lorentzian resonance both in its line shape and the basis of its occurrence. Unlike the Lorentzian resonances that can be described by a damped simple harmonic oscillator system, the Fano resonances that appear due to destructive interference of the broad continuum resonances with the discrete states are modeled by two coupled oscillator system. The physics of Fano resonance was first given by Ugo Fano,[1] while explaining the spectra of the autoionizing states of helium atoms. Since then there have been enormous interest in studying the Fano resonances in quantum as well as in the classical systems that include plasmonic nanostructures [2-4] and metamaterials.[5-7]

In metamaterials (MMs), Fano type spectral resonances are merely excited by altering the symmetry of the structure with respect to the incident field polarization axis. Fano resonances in MMs offer enhanced electric field confinements that are useful in probing the nonlinear effects[8,9] and in ultrasensitive sensor applications.[10] So far there here have been few experiments on tailoring the intensity and *Q*-factors of these Fano resonances by changing the asymmetry parameter or the coupling distance within the unit cell of the MM structure.[11-14] Recently, the effect of conductivity on the Fano resonance was probed, where the strength of Fano resonance could be tuned by choosing different materials as the resonators in the lower asymmetry regime. [15,16] These studies were focused on optimizing the Fano resonance

strength by altering the geometry of the MM structures in a passive scheme. However, judiciously integrating them with dynamic materials would provide an additional control in precisely manipulating the resonance properties of MM with the help of external stimulus.[17-21] For example, micro-electro-mechanical systems (MEMS)[22-24] are used to actively tune the near field coupling by voltage or by thermal actuation. However, it requires sophisticated fabrication facilities compared to the conventional photolithography techniques used in the micro-scale fabrications. On the other hand by integrating the MM with the photoactive materials [25-30] such as silicon has shown the active modulation of resonance properties in the MM system in a desirable fashion. In this work, we demonstrate active photo-switching of sharp Fano resonances in silicon implanted terahertz asymmetric metallic split ring (Si-TASR) resonator structure. Our results show complete modulation in the strength of the Fano resonance at very low pump powers. We employ a simple electrical circuit model to describe the coupling nature in the photo-excited Fano MM system that agrees well with the observed results.

II. Results and Discussion

To enact the active control of the Fano resonances in the Si-TASR structure, we fabricated the MM samples using two step photolithography processes. First, the desired TASR pattern was structured on Silicon-on-Sapphire (SoS) wafer using the conventional photolithography technique, where 200 nm thick aluminum metal was deposited on a SoS wafer comprising of 600 nm thick silicon epilayer and 460 μm thick sapphire substrate. As a second step of photolithography process, a positive photo-resist was placed in the gaps of the TASR structure and the reactive ion etching (RIE) process was performed to remove the undesired silicon from the substrate (detailed description on the fabrication can be found in supporting information). **Figure 1(a)** shows the graphical representation of the Si-TASR MM sample illuminated by a femtosecond optical pump beam and the terahertz probe beam. As the pump

beam illuminates the Si-TASR array, silicon at the gaps undergoes a change in its conductivity that gradually alters the strength of the Fano resonance. Figure 1(b) depicts the optical microscopy image of the fabricated sample with the unit cell dimensions as shown in the inset of the Figure. Asymmetry in the structure is introduced by displacing one of the two capacitive split gaps from the center by x = 15 μm within the TASR and the system asymmetry is quantified by the asymmetry parameter α, which corresponds to the difference in the lengths of the two metallic wires that forms the TASR structure [12]. By incorporating the silicon in the gaps of the asymmetric split ring resonators, we can actively control the photoconductivity of the silicon in response to the photo-excitation of the free carriers under the pump illumination, in-turn altering the effective field strength of Fano resonance in the gap of the structure.

Optical characterization of the Si incorporated TASR structure is performed using the Optical-pump and THz-probe (OPTP) spectroscopy setup, wherein femtosecond optical pump beam of wavelength 800 nm is incident on the surface of MM sample and the photo-response of the dressed sample is probed using the normal incidence of THz pulse that has a beam diameter of 3 mm. THz probe is derived from nonlinear generation using the ZnTe crystal via optical rectification process and is detected using the electro-optic sampling technique. The pump beam is derived from the amplified pulsed laser of pulse width ~ 120 fs and repetition rate of 1 kHz and has a beam diameter of 6 mm at the sample surface to ensure uniform photo-excitation of the silicon in the MM array. During the measurements, THz beam is delayed by 12 ps with respect to the pump pulse, where the free carrier density of the photo-excited silicon is the maximum.

Figure 2(a) shows the experimental results depicting the transmission response of the Si-TASR MM for the incident THz beam polarized perpendicular to the gaps ($\boldsymbol{E}_y$) for increased

power of the pump laser. Black curve represents the transmission response for the Si-TASR MM without the photo-excitation of the implanted silicon. We observe a strong Fano-type asymmetric line-shaped transmission resonance centered around 0.55 THz due to the larger asymmetry of the system, quantified by the asymmetry parameter α = 12.82% . The observed Fano resonance in the Si-TASR system is due to Fano type destructive interference between the broad dipolar metamaterial resonance (acts as a bright mode) and the sharp discrete mode that results from the asymmetry (x = 15 μm) in the structure (behaves as a dark mode). [5,12] When the Si-TASR MM is illuminated by the pump beam of 1 mW power (fluence = 3.5 μJ/cm^2), strength of the observed Fano resonance weakens, as shown by the red curve in Figure 2(a). Upon further increase in the pump power, Fano resonance amplitude in the system abates gradually with minimal shift in the resonance frequency and it completely disappears when the excitation pump power is increased to 40 mW (fluence = 140 μJ/cm^2). The observed amplitude modulation of the Fano resonance is associated with the change in the photoconductivity of the silicon implanted in the gaps of the Si-TASR structure. As we increase the pump power, the number of photo-excited carriers in silicon increases that in-turn increases its conductivity. Hence, silicon, which is a semiconductor at terahertz frequencies, behaves like a quasi-metal at increased pump powers with a skin depth of around 8 μm at 1 THz for a pump power of 40 mW. This change in the behavior of silicon shorts the capacitive split-gaps leading to the complete switch-off of the Fano resonance feature in the Si-TASR MM array. Here, we would like to highlight that the pump power used to switch off the Fano resonance is nearly 20 times lower than the results reported in previous studies.[28,29] This demonstrates the sensitive nature of ultra-sharp Fano resonances to the external stimulus. We have performed the high resolution numerical simulations for the ultra-sharp Fano resonance with lower asymmetries (α = 2.5% and α = 6.8%) and we found that the pump power required for switching-off the high-Q Fano resonance is extremely low, which is about 1 mW and 12

mW for Fano resonators with α = 2.5% and 6.8 %, respectively. These low power switching-off of the high *Q* resonances manifest the ultra-sensitive nature of these resonances to the external perturbation. A more detailed description is provided in the supporting information.

To study the nature of the photo-excitation mediated modulation of the Fano resonances, we employed the numerical simulations using commercially available CST Microwave Studio frequency domain solver that is based on the finite integration technique. We examined the frequency response of the Si-TASR unit cell, by choosing lossy aluminum metal with σ_{dc} = 3.56×10^7 S/m as TASR resonators and sapphire (ε_r = 10.5) as a transparent substrate. Silicon (ε_r = 11.7) was placed beneath the metallic TASR resonators (as shown in the Figure 1(a)) and the conductivity of silicon was varied to observe the modulation in the strength of Fano resonances. While conducting our experiments, we ensured that the pump light is illuminated from the front side of the sample such that the 800 nm pump light does not see the silicon beneath the 200 nm thick metallic layer. Therefore, we would like to stress that the silicon present in the split gap rather than the part beneath the metal is responsible for the active photo-switching of the Fano resonance. In the simulations, the conductivity of silicon was modeled by experimentally obtained real part of the photo-conductivity data for the corresponding powers of the excitation pulse (given in Figure 2(a)). Photo-conductivity of the silicon was determined by the OPTP measurements, by photo-exciting the silicon epilayer on sapphire (SoS) for different pump powers (1 mW to 40 mW). Measurements were performed by alternatively scanning the THz pulse through the photo-excited SoS wafer and the bare sapphire substrate for different pump powers. In the post processing steps, the measured transmission response through SoS is normalized to the bare sapphire substrate and the photo-induced conductivity of the silicon layer alone is extracted using the optical constants extraction formula.[31]

As shown in Figure 2(b), the simulated spectra for varying conductivity of silicon show good agreement with our experimental results. Pump powers shown in the Figure 2(a) correspond to the conductivity values of the silicon (Figure 2(b)) that are extracted from the OPTP measurements. In other words, the photoconductivity of silicon is proportional to the illuminating pump power. The intriguing feature of the observed results is that the modulation of Fano amplitude occurs at very low powers of the excitation pulse (low photoconductivity of silicon) as compared to similar studies performed on other metamaterial resonances.[27-29] This critical behavior of Fano resonances shows the ultrasensitive nature of its near fields to the external stimulus over other kind of metamaterial resonances. In the absence of the pump beam, the Si-TASR structure shows maximum confinement of the electric field in the gaps at the Fano resonance frequency, as shown in **Figure 3(a)**. This is because the gaps in the structure create the capacitance effect, where the charges due to the oscillating current accumulate and enhance the field strength within the gaps. With increasing free carriers in the silicon, the photoconductivity of silicon starts to increase and that gradually diminishes the capacitance effect at the Si-TASR gaps. When the pump power is increased to 40 mW (fluence = 140 $\mu J/cm^2$), the capacitance effect completely vanishes (shown in Figure 3(b)) in the system giving rise to a dipole nature of the resonance in the structure. The resonance switching behavior can be further understood and clearly seen by the nature of surface currents on the Si-TASR structure at the Fano resonance frequency, shown in the Figures 3(c) and 3(d). Without pump, Si-TASR structure excites the anti-parallel (out-off phase) currents at the Fano resonance frequency, which signifies the magnetic nature of the resonance with the magnetic dipoles oriented perpendicular to the structure plane. By shining the pump beam of 40 mW power, the nature of the currents are switched from anti-parallel to parallel (in-phase) behavior, where the Fano dip completely disappears. Thus, by changing the photoconductivity of silicon, capacitance in the gap of the Fano resonators can be completely switched-off at moderate pump powers. This would enhance its practical applications in

designing the ultrasensitive active sensors and resonance based ultrafast switching devices for terahertz communication.

We further extend our analysis to quantitatively describe the modulation of the Fano resonance with change in the photoconductivity of silicon. We define a quantity called Figure of Merit (FoM), which is a product of the *Q*-factor and the resonance intensity (ΔI) (FoM = $Q \times \Delta I$) that quantifies the strength of Fano resonance. Its behavior with respect to the external perturbations determines the nature of near field coupling in the Fano system. In our previous study[12] on passive tailoring of Fano resonances, we show that the variation in the FoM follows a peak function, wherein the rising slope is dictated by the exponentially increasing Fano intensity and the fall-off behavior is majorly dictated by the exponentially declining *Q*-factors. These observations focused on modulating the strength of Fano resonance by changing the asymmetry parameter (α) in a passive way. However, in the present work, the strength of the Fano resonance is actively tuned by changing the structural properties of the resonator through photo-excitation/photo-doping the silicon placed in the gaps of the Si-TASR structure. Unlike the passive studies, the active modulation through photo-doping shows an exponential decay in Fano resonance strengths (FoM) with increasing photo-conductivity of the silicon, as shown in **Figure 4(a)**. A simple electrical circuit model is employed to elucidate the observed exponential behavior in the FoM with increasing photoconductivity of the silicon placed in the gaps of the Si-TASR MM resonators. The Si-TASR MM system can be analogous to the capacitor circuit, wherein two gaps act as capacitors and the silicon placed in the gaps is modeled as a dielectric material with $\varepsilon_r = 11.7$. The equivalent circuit diagram for the Si-TASR system is given in Figure 4(b), where the gap in the structure acts as a capacitor, and the photo-doped silicon acts as a variable resistor. The observed exponential decrease in the FoM with increasing photo-conductivity is a consequence of the charge discharging effect in the capacitor circuit, where the charges decay

via resistor-capacitor loop and hence decreasing the net capacitance in the system. In the absence of optical pump, as the THz pulse incident on the Si-TASR sample, electric field (v_c) builds up in the gaps, which results in the net capacitance within the system (see Figure 3(a)). Whereas, in the presence of optical pump, enhancement of the pump power leads to an increase in the conductivity (inverse of resistivity) of the silicon patch within the gap of the Si-TASR structure. Hence, the enhanced photoconductivity of silicon gradually shorts the capacitor gap and the electric field accumulated in the capacitor gap discharges exponentially that explains the observed exponential behavior of the strength (FoM) of the Fano resonance. The relation between the conductivity and the electric potential stored in the Fano resonator gaps is given by the expression,

$$v_c = V e^{-R_0 \sigma} \quad [1]$$

where, v_c is the electric potential in the capacitive gaps, σ is the silicon conductivity, V is the input voltage and R_0 is a constant that depends inversely on the permittivity (ε_r) of the dielectric material and has a SI unit of $F^{-1}\cdot m\cdot s$. The variation of v_c with conductivity (σ) is fitted to the FoM variation, which agrees very well with both simulated and measured data, as shown in the Figure 4 (a). Detailed derivation of **Equation 1** is given in the supporting information under theoretical calculations section. Thus, electric field in the resonator gap (capacitor) shows an exponential decay with respect to increasing conductivity of the silicon patch and hence gradually weakens the strength of Fano resonance in the system. As shown in Figure 4(b), the Fano coupling in the asymmetric MM resonators mimics the electrical response in a basic RC circuit driven by an external voltage.

III. Conclusion

In conclusion, we have demonstrated active photo-switching of the Fano resonances in a silicon implanted Fano resonator (Si-TASR) structures. Our results manifested the ultrasensitive nature of the Fano resonances, which can be switched off at very low optical

pump powers. We also discovered that the strength of the Fano resonance, quantified by FoM values showed an exponential decay with the increase in the photoconductivity of the silicon. This behavior was analogous to the discharging of the capacitor in a simple RC electrical circuit model and showed an excellent agreement with our observed results. Besides revealing the coupling phenomenon in the Fano resonators, our results show a new and promising way to design active sensors, low threshold switching in metadevices and have the potential to provide a precise active control on the nonlinearity offered by the highly sensitive Fano resonances.

IV. Acknowledgement

We acknowledge the research funding support from NTU startup Grant No. M4081282, Singapore MOE Grant Nos. M4011362, M4011534, MOE2011-T3-1-005, and MOE2015-T2-2-103.

V. Supporting Information

Supporting Information is available online from the Wiley Online Library or from the author.

References

1. Fano, U., *Phys. Rev*. **1961**, 124, 1866–1878.
2. Boris luk'yanchuk, Nikolay I. Zheludev, Stefan A. Maier, Naomi J. Halas, Peter Nordlander, Harald Giessen and Chong Tow Chong, *Nat. Mater.*, **2010**, 9, 707-715.
3. Andrey E. Miroshnichenko, Sergej Flach, and Yuri S. Kivshar, *Rev. Mod. Phys*. **2010**, 82, 2257-2298.
4. Vincenzo Giannini, Yan Francescato, Hemmel Amrania, Chris C. Phillips, and Stefan A. Maier, *Nano Lett*. **2011**, 11 (7), 2835–2840.

5. Fedotov. V. A, Rose M, Prosvirnin. S. L, Papasimakis N., and Zheludev. N. I. *Phys. Rev. Lett*. **2007**, 99**,** 147401.
6. C. Wu, A. B. Khanikaev, R. Adato, N. Arju, A. Ali anik, H. Altug, and G. Shvets**,** *Nature Mater.*, **2012**, 11, 69–75.
7. R Singh, I. A. I. Al-Naib, M. Koch, and W. Zhang, *Optics Express*, **2011**, 19 (7), 6312-6319.
8. M. Kroner, A. O. Govorov , S. Remi, B. Biedermann, S. Seidl, A. Badolato, P. M. Petroff, W. Zhang, R. Barbour, B. D. Gerardot, R. J. Warburton, and K. Karrai, *Nature*, **2008**, 451, 311-314.
9. N. I. Zheludev, S. L. Prosvirnin, N. Papasimakis, and V. A. Fedotov, *Nature Photonics*, **2008**, 2, 351-354.
10. R. Singh, W. Cao, I. Al-Naib, L. Cong, W. Withayachumnankul, W. Zhang, *Appl. Phys. Lett.*, **2014**, 105 (17), 171101.
11. R. Singh, I. Al-Naib, W. Cao, C. Rockstuhl, M. Koch, W. Zhang, IEEE Transactions on Terahertz Science and Technology **2013**, 3 (6), 820-826.
12. L. Cong, M. Manjappa, N. Xu, I. Al-Naib, W. Zhang, R. Singh, *Adv. Opt. Mater.* **2015**, 3, 1537.
13. Peter Offermans, Martijn C. Schaafsma, Said R. K. Rodriguez, Yichen Zhang, Mercedes Crego-Calama, Sywert H. Brongersma, and Jaime Gomez Rivas, *ACS Nano*, **2011**, 5, 5151.
14. G. Dayal, X.Y Chin, C. Soci, R. Singh, *Adv. Opt. Mater*. **2016**. DOI: 10.1002/adom.201600417.
15. Y.K Srivastava, M. Manjappa, L. Cong, W. Cao, I. Al-Naib, W. Zhang, R. Singh, *Adv. Opt. Mater*. **2015**, 4, 457–463.
16. Y.K Srivastava, M. Manjappa, H.N.S. Krishnamoorthy, R. Singh, *Adv. Opt. Mater*. 2016. DOI: 10.1002/adom.201600354.
17. R. Singh and N. Zheludev, *Nat. Photon.* **2014**, 8, 679–680.

18. Chihun In, Hyeon-Don Kim, Bumki Min, Hyunyong Choi, *Adv. Opt. Mater*. **2016**, 28 (7), 1495-1500.
19. Wei-Shun Chang, J. Britt Lassiter, Pattanawit Swanglap, Heidar Sobhani, Saumyakanti Khatua, Peter Nordlander, Naomi J. Halas, and Stephan Link, *Nano Lett*. **2012**, 12, 4977−4982.
20. R. Singh, A. K. Azad, Q. X Jia, A. J. Taylor, and H.-Tong Chen, *Opt. Lett*. **2011**, 36, 1230-1232.
21. Savo S., Shrekenhamer D. and Padilla W. J., *Adv. Opt. Mater*. **2014**, 2, 275–279.
22. Tao H., Strikwerda A. C., Fan K., Padilla W. J., Zhang X, and Averitt, R. *Phys. Rev. Lett*. **2009**, 103, 147401.
23. W.M. Zhu, A.Q. Liu, T. Bourouina, D.P. Tsai, J.H. Teng, X.H. Zhang, G.Q. Lo, D.L. Kwong, and N.I. Zheludev**,** *Nat. Commun*. **2012**, 3, 1274.
24. P Pitchappa, M Manjappa, CP Ho, R Singh, N Singh, C Lee, *Adv. Opt. Mater.* **2016**, 4, 541–547.
25. Padilla W. J., Taylor A. J., Highstrete C., Lee M., and Averitt R. D., *Phys. Rev. Lett*. **2006**, 96, 107401.
26. S. Zhang, J. Zhou, Y-S. Park, J. Rho, R. Singh, S. Nam, A. K. Azad, H.-T. Chen, X. Yin, A. J. Taylor, and X. Zhang, *Nature comm*. **2012**, 3, 942.
27. H. –T. Chen, J. F. O'Hara, A. K. Azad, A. J. Taylor, R. D. Averitt, D. B Shrekenhamer, and W. J. Padilla. *Nat. Photon*. **2008**, 2, 295–298.
28. Jianqiang Gu, Ranjan Singh, Xiaojun Liu, Xueqian Zhang, Yingfang Ma, Shuang Zhang, Stefan A Maier, Zhen Tian, Abul K Azad, Hou-Tong Chen, Antoinette J Taylor, Jiaguang Han, and Weili Zhang, *Nature Commn*. **2012**, 3, 1151.
29. Dibakar Roy Chowdhury, Ranjan Singh, Antoinette J. Taylor, Hou-Tong Chen, and Abul K. Azad, *Appl. Phys. Lett*. **2013**, 102, 011122.

30. I. Chatzakis, L. Luo, J. Wang, N.-H. Shen, T. Koschny, J. Zhou, and C. M. Soukoulis, *Phys. Rev. B.* **2012**, 86, 125110.

31. Ronald Ulbricht, Euan Hendry, Jie Shan, Tony F. Heinz, and Mischa Bonn, *Rev. Mod. Phys.* **2011**, **83**, 543-586.

Figures

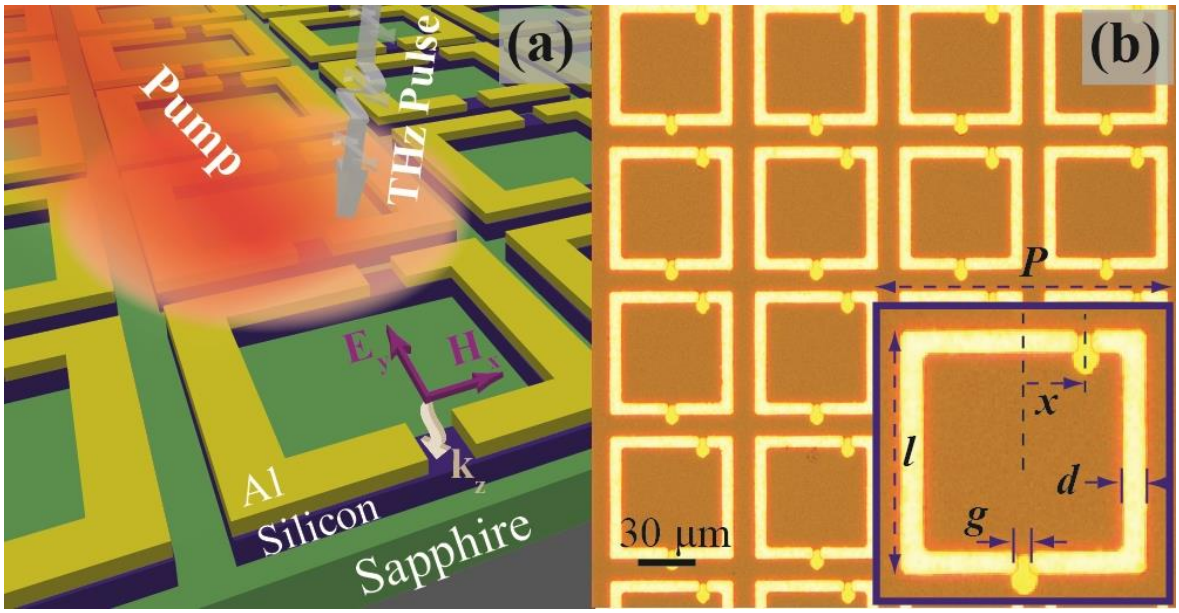

Figure 1. (a) Graphical representation of the Si-TASR MM sample under the optical pump and THz probe illumination. **(b)** Optical Microscopy (OM) image of the Si-TASR sample showing the silicon islands at the split gaps. Inset figure shows the unit cell dimensions of the Si-TASR structure with lattice periodicity, *P*: 70 μm; resonator length, *l*: 60 μm; asymmetry distance, *x*: 15 μm; gap, *g*: 3 μm; and the resonator width, *d*: 6 μm.

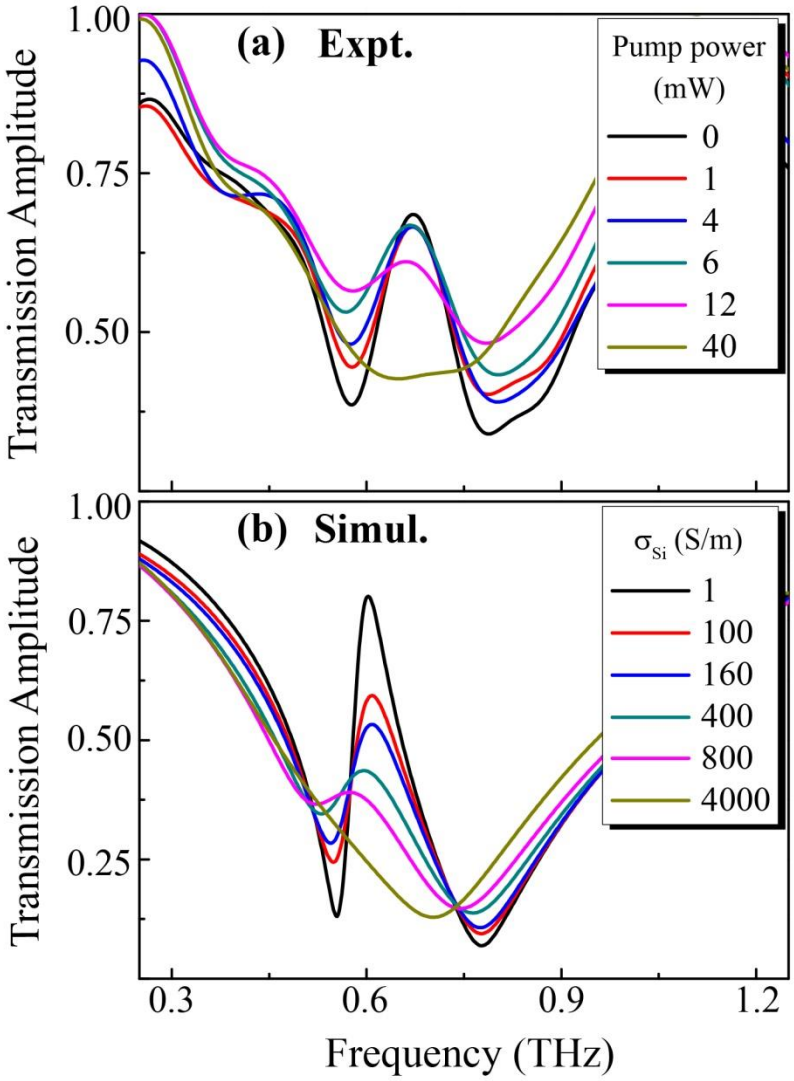

Figure 2. **(a)** Experimental results showing the active modulation of Fano resonances at 0.58 THz for varying optical pump power. **(b)** Simulation curves justifying our experimental results. The conductivity values σ_{Si} for silicon shown in part **(b)** are proportional to the pump powers shown in part **(a)**.

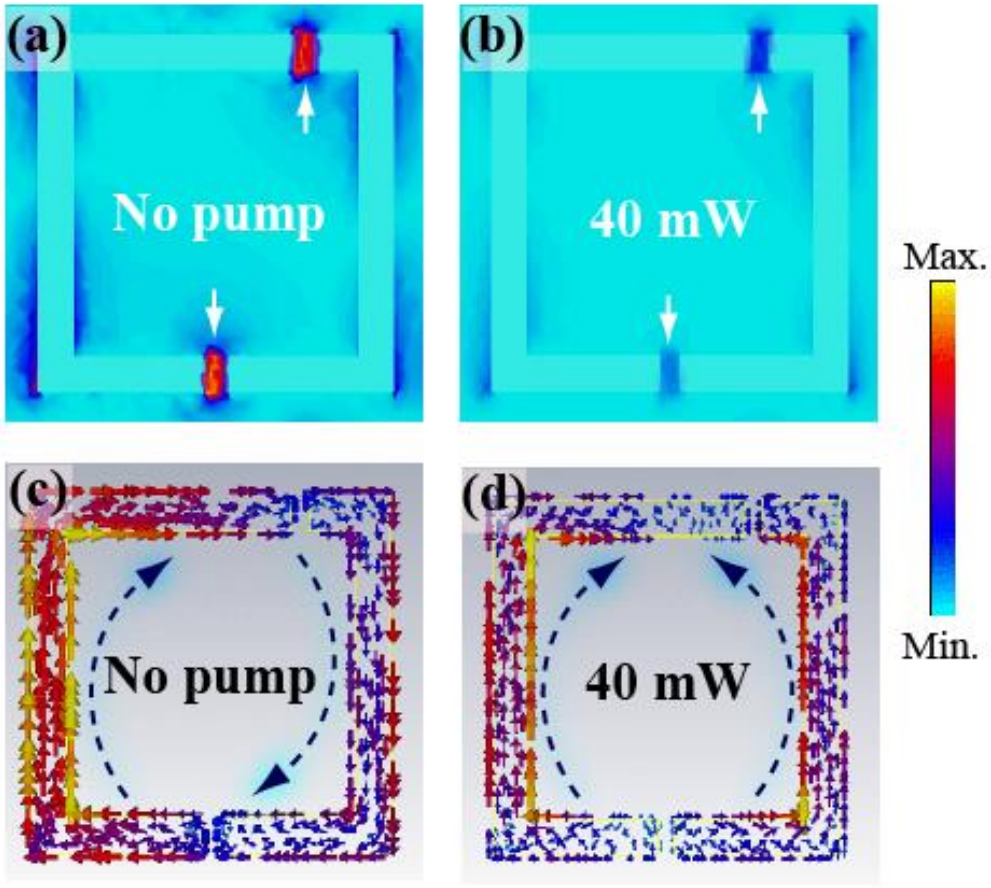

Figure 3. **(a)** and **(b)** Depicts the electric field strengths at the Fano resonance dip, without and with the photo-excitation of the samples, respectively. As shown, the electric field at the resonator gap switches off in the presence of 40 mW pump beam. **(c)** and **(d)** Show the corresponding surface current distributions at the Fano resonance dip that reveals the active switch in the nature of surface currents from the anti-parallel to parallel currents, after the photo excitation of the sample by 40 mW pump beam.

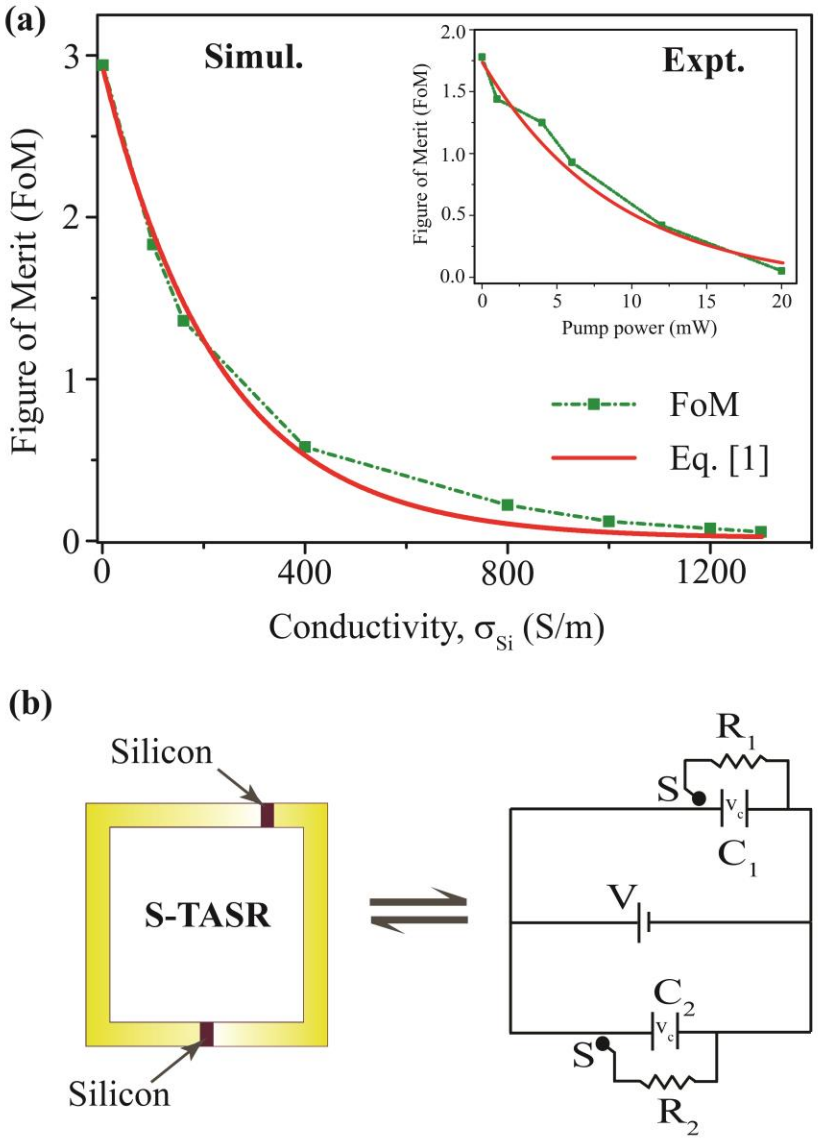

Figure 4. **(a)** Figure of Merit (FoM) variation of the Fano resonances with respect to the conductivity of silicon. The red curve provides the theoretical fit to the observed results using the electrical circuit model given by the equation [1]. **(b)** Equivalent electrical circuit model for the studied Si-TASR MM resonator, where the capacitors with capacitance $C_1 = C_2 = C$ in the electrical circuit corresponds to the capacitance gaps in the MM structure and the resistors with resistance $R_1 = R_2 = R$ corresponds to the photo-excited silicon patches that acts as a lossy channel in the given electrical circuit. S is the switch, V is the applied voltage and v_c is the electric potential in the capacitor gap.

Supporting Information

Active Photo-switching of sharp Fano resonances in THz metadevices

Manukumara Manjappa[1,2,], Yogesh Kumar Srivastava[1,2,*], Longqing Cong[1,2,*], Ibraheem Al-Naib[3], and Ranjan Singh[1,2,†]*

Fabrication Process: Si-TASR metamaterial structures were fabricated on a Si-on-Sapphire (SoS) wafer comprised of 600 nm thick undoped Si film on a 460 μm thick sapphire substrate. In the first step of photolithography process a positive photo-resist was coated on SoS wafers and wafers were prebaked at 100 ^{0}C for 1 minute. Later on the wafers were exposed under UV light by covering with an appropriate mask. Desired structural pattern were obtained by soaking the wafers in the developer solution by removing the unexposed part of the photo-resist. Once the pattern was ready, 200 nm thick aluminum was deposited using thermal evaporation method and liftoff was performed by soaking the structure in acetone for two days to get the desired structures. The second step photolithography was performed using same positive photo-resist to cover the split gap, followed by RIE to etch off undesired Si. Wafers were finally soaked in acetone to remove photo-resist and to get desired metamaterial structure as shown in Figure 1.

Theoretical Calculations: Analogy of the Si-TASR MM structure to the RC electrical circuit was established by deriving an expression for the electric potential in the resonator gaps by using the capacitor discharge equation given for the RC electrical circuit. The RC discharging expression is given by,

$$v_c = V e^{\frac{-t}{\tau}} \quad [2]$$

Expressing the time constant ($\tau = R \bullet C$) in terms of the conductivity (σ) and the dielectric permittivity (ε_r), the electric potential in the capacitor gap at time t_0 is expressed as,

$$v_c = V e^{-\frac{t_0 A_1 g}{l \varepsilon_r A_2} \bullet \sigma} = V e^{-R_0 \bullet \sigma} \quad . \qquad [3]$$

Where, l and A_1 are the length and the cross section area ($A_1 = l \times d$) of the resonator arm; g and A_2 are the separation and area ($A_2 = g \times d$) of the capacitor gap. ε_r is the permittivity of the implanted silicon. R_0 is a constant that depends inversely on the permittivity of the dielectric material implanted in the capacitors gap.

Pump influence on high *Q* Fano resonances: High *Q* resonances are challenging to measure in the ZnTe based Optical-pump Terahertz-probe (OPTP) measurements due to reflection in the system. Hence, we provide numerically obtained results on the influence of pump powers on the ultra-sharp Fano resonances at lower asymmetries of the system. The numerical simulations were carried out using CST microwave studio with the same material parameters as discussed in the main manuscript. The Fano resonators with structural asymmetries of α = 2.5 % (x = 3 μm) and α = 6.8 % (x = 8 μm) are considered for the simulation. The asymmetry parameter is defined as the difference between the lengths of the two metallic wires that forms the TASR structure and is given by $\alpha = \frac{(l_1 - l_2)}{(l_1 + l_2)} \times 100\ \%$, as shown in the **Figure S1** (a). The transmission response of the Fano resonances due to the change in the photoconductivity of silicon for asymmetries α = 2.5 % and α = 6.8 % are shown in **Figure S1 (a) and (b)**, respectively. It is clearly seen that, as the *Q*-factor of the Fano resonance increases at lower asymmetries, it becomes extremely sensitive to the external perturbations. For instance, Fano resonance at asymmetry α = 2.5 % shows maximum sensitivity to the external pump, where the resonance can be switched-off at very low optical pump power of about 1 mW (σ_{Si} = 100 S/m), as shown by Figure S1(a). Whereas, in the case of higher asymmetries, for example α = 6.8 % the required pump power to switch-off the Fano resonance increases to 12 mW (σ_{Si} =

800 S/m), as shown in the Figure S1(b). These pump powers are almost two to three orders of magnitude lower compared to the pump powers required to switch-off the EIT type of resonances and LC resonances reported in previous works. Such low power modulation of Fano resonances could be pivotal in realizing low threshold active nonlinear devices, phase and amplitude modulators and could trigger the pathways for achieving the active sensors for biological applications.

The variation in the Figure of Merit (FoM) for the Fano resonances at asymmetry α = 2.5 % and α = 6.8 % under the photo-excitation of the silicon is depicted in **Figure S2 (a) and (b)**, respectively. The variation follows the exponential decay and exhibit similar behavior observed for the Fano resonator at α = 12.85 % (discussed in the manuscript). The curves are fitted with the function described by **Equation. 1** of the main manuscript that shows excellent agreement between results obtained from the theoretical expression based on a RC electrical circuit model and the observed results. Thus, the behavior in the variation of near field coupling under the pump illumination is similar for all the Fano asymmetries, although their sensitivity shows a drastic change.

Supporting Information Figures:

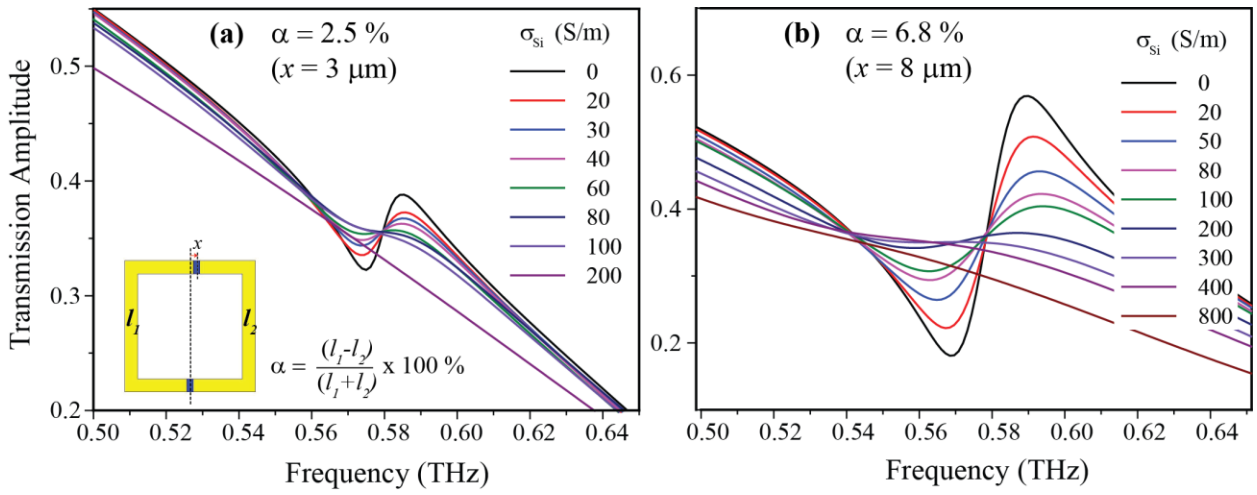

Figure S1. Numerically simulated transmission spectra depicting the modulation of the Fano resonance in the metamaterial sample with asymmetry **(a)** α = 2.5 % and **(b)** α = 6.8 % for a

sweep of silicon conductivity. The pump power corresponding to the conductivity values are for 0 S/m = 0 mW; 100 S/m = 1 mW; 400 S/m = 6 mW; and 800 S/m = 12 mW.

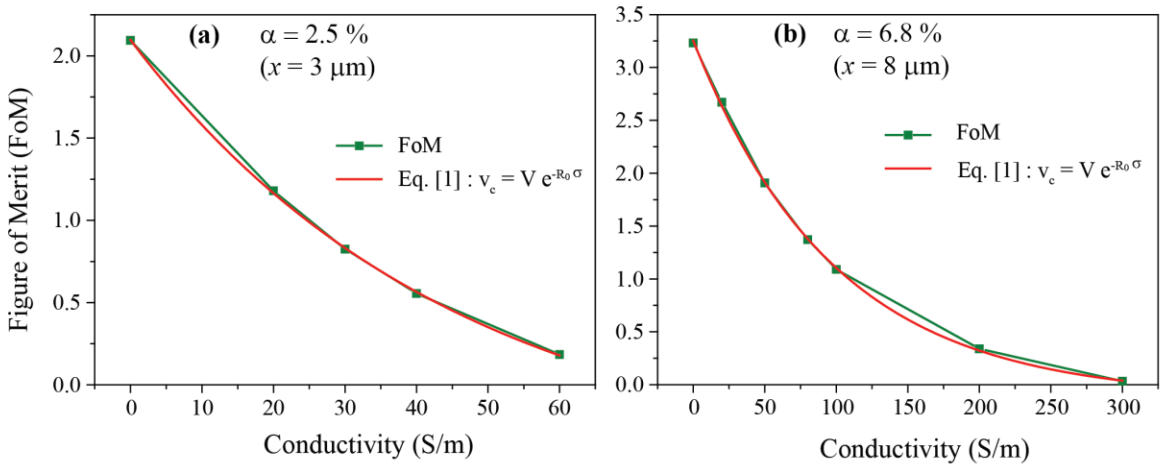

igure S2. Figure of Merit variation obtained for the numerically simulated Fano curves at **(a)** α = 2.5 % and **(b)** α = 6.8 % for a sweep of silicon conductivity. The red curve shows the theoretical fit with Eqn. [1] of the main manuscript.